Proc. Natl. Acad. Sci. USA.
Vol. 75, No. 8, pp. 3751–3755, August 1978
Biophysics

Matrix protein from *Escherichia coli* outer membranes forms voltage-controlled channels in lipid bilayers

(association of vesicle-spread monolayers/quantitative protein incorporation/negative resistance/protein–protein interaction/glucose permeability)

HANSGEORG SCHINDLER AND JURG P. ROSENBUSCH

Biozentrum, University of Basel, CH-4056 Basel, Switzerland

Communicated by Bernard D. Davis, May 22, 1978

ABSTRACT **Matrix protein from *Escherichia coli* was integrated into planar lipid bilayers. The incorporated protein generates aqueous channels across these membranes. Channels are induced irreversibly by voltage, and their number is proportional to the protein content of the membrane and stays constant over hours. They are uniform in size, with a diameter of about 1 nm and a single-channel conductance of 0.14 nS in 0.1 M NaCl. In addition to ionic conductance, the channels allow free diffusion of small, uncharged molecules. Channels assume either an open or a closed state. Membrane potentials shift this two-state equilibrium distribution in favor of closed channels, an observation that explains both negative resistance and inactivation at high potentials. Channels are not randomly distributed in the membrane but interact cooperatively within aggregates. The smallest entity inducible consists of three channels.**

Matrix protein from *Escherichia coli*, which is identical to porin (1) or PG1 (cf. ref. 2), spans the outer membrane of the cell (for a review see ref. 3). It has recently been shown (1) to account for the molecular sieving properties of this structure (4). The protein consists of a single polypeptide (M_r 36,500), and the 10^5 molecules per cell are arranged in a single layer in the bacterial envelope in a highly periodic array (5) which exhibits 3-fold symmetry and triplet indentations that have tentatively been interpreted as pores (6). Pertinent in the present context is that matrix protein binds detergents only weakly in its native form and that it is highly insoluble in aqueous solutions (5, 7). In contrast, solvents such as benzene or toluene dissolve it without causing disaggregation or denaturation (7).

Reconstitution of active proteins into single bilayer lipid vesicles has substantially contributed to the understanding of membrane function (8). That integration of transmembrane proteins into planar lipid bilayers has not been as successful has been attributed to the failure of many proteins to interact with preformed membranes, as well as to deleterious effects of residual detergents and hydrocarbon solvents (9). Due to the properties mentioned above, matrix protein appeared an obvious choice for integration into lipid bilayers. We have used its successful incorporation into vesicles (1) as a first step in the formation of planar lipid bilayers. Monolayers formed from vesicles in the absence of residual detergents, hydrocarbon solvents, membrane doping agents, or added lipopolysaccharides were subsequently converted to bilayers. In this report, we show that matrix protein induces voltage-dependent channels in planar membranes. The analysis of their electrical properties as well as tracer flux experiments provide functional assays that may contribute to a better molecular understanding of its function.

The costs of publication of this article were defrayed in part by the payment of page charges. This article must therefore be hereby marked "*advertisement*" in accordance with 18 U. S. C. §1734 solely to indicate this fact.

MATERIALS AND METHODS

Matrix protein was prepared from *E. coli* BE by sequential enzymatic hydrolysis of envelopes with lysozyme, nucleases, and trypsin (7), followed by differential heat extraction (5) and gel filtration on Sepharose 4B in the presence of 0.1% dodecyl sulfate. After repeated washings, carrier-free dodecyl [^{35}S]-sulfate (10^5 cpm) was added to the purified protein, which was then chromatographed on Sephadex G-75 in 0.2 mM dithiothreitol. It eluted in the exclusion volume with <2 mg of detergent per g of protein. Quantitation (6) of contaminating lipoprotein [which is unlikely to affect (1) the results presented here] showed ≤0.1 mol/mol of matrix protein. Labeled preparations were obtained (10) from cells grown to late exponential phase in the presence of a ^{3}H-labeled amino acid mixture [all radiochemicals were from Amersham (England)]. The native state (7) of matrix protein at pH 10 in B buffer (10 mM K_2CO_3-$KHCO_3$, 0.1 M KCl) was ascertained by the heat dependence of its electrophoretic mobility and its protease resistance (5). Dioleoylphosphatidylcholine was synthesized (11), analyzed for purity (12, 13), and quantitated (14) as described. Phospholipid vesicles were made (15) in A buffer (1 mM *N*-2-hydroxyethylpiperazine-*N'*-2-ethanesulfonate/0.1 M NaCl) at pH 7.4 in the presence of 10 mM $MgCl_2$ and 1 mM NaN_3.

^{3}H-Labeled matrix protein was added to preformed vesicles and incorporated by sonication in an MSE (London) sonifier (1 min, position 7). Protein-to-lipid ratios were obtained from the specific radioactivity of ^{3}H-labeled matrix protein and from phosphate determinations (14). Because these ratios are identical in the mixture before sonication and in purified vesicles, high-speed centrifugation or gel filtration could be dispensed with, allowing quantitative recovery.

Freshly sonicated, single bilayer vesicles [monitored by coherent light scattering (16)] were spread onto an air–water interface (17). The resulting monolayers (unpublished data) were characterized in a Langmuir balance (18), and the conditions were optimized for subsequent bilayer formation. The final equilibrium surface pressures were within 20–40 dyne/cm, depending on the protein concentration. Their identity as monolayers was ascertained by surface pressure/area curves (18) after dislocation to a compartment not containing vesicles. Protein-to-lipid ratios were determined after withdrawal of the monolayer from that compartment. The minimal amount of vesicles needed to achieve formation of condensed monolayers within minutes was 0.5–2 μg of lipid vesicles per cm^2. Monolayers were then formed in the two compartments of a membrane cell (19) with surface areas of 1.2 cm^2 each. Water phases on both sides consisted of A buffer for pH values 6–8 and B buffer for pH 9.2–10.

The two monolayers, one obtained from pure lipid vesicles and the other from vesicles containing matrix protein, were

subsequently combined to a bilayer (20) by apposition over a circular aperture which was pretreated with petroleum jelly. The surface area of the bilayer was 0.02 mm^2, and the temperature was 22°.

Current and capacitance measurements were performed as described (19). The sign of electrical potentials always refers to the compartment to which protein-containing vesicles were added. The bandwidth of fluctuation measurements was 3 kHz unless indicated otherwise. In a control experiment, protein-containing vesicles were applied to one compartment of a membrane cell separated by a pure phospholipid bilayer that was formed from hexane-spread monolayers (20). In this instance, no conductance (cf. *Results*) could be induced. This demonstrates that vesicles do not incorporate by fusion into preexisting membranes at the concentrations used.

RESULTS

The bilayer character of membranes formed from vesicle-spread monolayers was tested by the following criteria. Their specific capacitance was 0.7 ± 0.1 $\mu F/cm^2$ and their resistance was about 10^8 Ω-cm^2, values in excellent agreement with those obtained from bilayers formed from hexane-spread monolayers (19, 21). Also, trace amounts of gramicidin and alamethicin formed channels across the membranes that were indistinguishable from those recorded in conventional bilayers (19, 22). The success rate of bilayer formation was as high as with hexane-spread monolayers (19), and the membranes formed were routinely stable over 3–10 hr. Dielectric breakdown voltages exceeded 350 mV. Extraneous lipopolysaccharides were not added at any stage, but each mol of matrix protein contains 3 mol of lipopolysaccharide or at least their lipid moieties (23), in tight association (unpublished data). The results presented here were obtained with dioleoylphosphatidylcholine, and protein incorporation was asymmetric (cf. *Methods*). Dioleoylphosphatidylethanolamine and phosphatidylserine, as well as symmetrical protein incorporation, were also used and will be described in detail elsewhere.

Electrical membrane properties

Initiation of Conductance. At low potentials and at pH values between 6 and 8, membranes containing matrix protein did not show conductance beyond that observed in pure phospholipid bilayers. A delayed current response was seen (Fig. 1 *left*) when a membrane potential greater than V_i (as defined in the legend to Fig. 2) was applied. The total conductance induced during initiation increased with voltage. Initiation was dependent on pH (cf. legend to Fig. 2) and on protein concentration. Increasing numbers of steps, and consequently higher conductances, were observed with increasing protein-to-lipid ratios. Different ions (NaCl, KCl, $MgCl_2$, $CaCl_2$), and variation of ionic strength (0.01–1 M) appeared not to affect the initiation process. Initiation was irreversible because, after the voltage was set to zero, a renewed application of the same potential resulted in an immediate and highly reproducible current increase to a value corresponding to the sum of all individual initiation steps observed previously (instantaneous current). Large initial potentials (exceeding V_c, defined in the legend to Fig. 2) led to saturation and caused membranes to be fully induced. Such preinduced membranes were used for the following studies.

Steady-State Conductance. After initiation, the current reached a steady-state (Fig. 1 *right*). The dependence of the steady-state current on voltage is shown in Fig. 2*A* and exhibits a negative slope above 140 mV. The significance of this negative differential resistance will be discussed below. The relationship between conductance and voltage is characterized by a sigmoidal transition between two levels (15 and 2 nS in Fig. 2*B*). The dependence of the conductance on the protein concentration in the bilayer, determined at steady-state (Fig. 2*C*), shows an approximately linear relationship between molar stoichiometries of protein to lipid of 1:160,000 (1:3000; wt/wt), and 1:5200 (1:100 wt/wt).

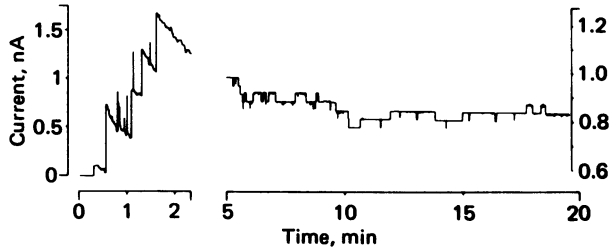

FIG. 1. Initiation of conductance in a matrix protein-containing membrane. A potential of 240 mV was applied at time 0 (15 min after membrane formation). The initiation process (*Left*) showed large current increases that appeared to be single events (time resolution, 0.3 msec). Each large increment was followed by a decay in small steps. The end of initiation and the steady-state are illustrated by the same trace (*Right*) on an enlarged scale; note also the different time scales. Individual step heights during steady-state are 33.5 ± 5.0 pA (0.14 ± 0.02 nS). The stepwise fluctuations at steady-state yield a standard deviation of ±0.1 nS (averaged over 120 steps during 60 min), as compared to a conductance level of 3.5 nS. At higher conductances (70 nS), standard deviations (always obtained by averaging over time periods exceeding at least by an order of magnitude the life-times of individual steps) were <±0.4 nS. The experiments shown here and in Figs. 2 and 3 were performed in A buffer at pH 7.4 with protein-to-lipid ratios of 1:500 (wt/wt).

Current Relaxation. Voltage application to preinduced membranes resulted in an instantaneous current rise to a value that is proportional (ohmic) to the potential applied (cf. instantaneous current-voltage curve in Fig. 2*A*). The relaxation from the instantaneous current to the steady-state level is illustrated in Fig. 3. During this inactivation, the current decay occurred in cascades of small steps. Relaxation times were voltage dependent. If, within the region of negative resistance, the voltage was lowered, a new steady-state current was attained that corresponded to that characteristic of the new potential, thereby demonstrating that the steady-state currents reached are independent of the pathway of approach. If, after the voltage was returned to zero, the same potential was applied again, a full-scale instantaneous current response was observed only after a recovery time of at least 2 sec at zero voltage (data not shown).

Conductance Steps. Conductance changes always occurred stepwise and were clearly resolved (Fig. 1 and 3), even at the highest conductance levels observed. At any given ionic strength, these conductance increments were uniform and independent of voltage, allowing the definition of a unit step of conductance. At 0.1 M NaCl, the ionic strength used routinely in this study, it was 0.14 ± 0.02 nS (cf. legend to Fig. 1). The dependence on ionic strength was linear within the region tested (0.01–1 M). Unit step height varied only slightly for different cations (1.4, 2.1, 2.4, and 2.6 nS for 1 M NaCl, KCl, RbCl, and CsCl, respectively), indicating poor cation selectivity. At high conductance levels, fluctuations occurred within narrow limits (Figs. 1 and 3). This resulted in standard deviations that are small compared to the conductance levels (e.g., ±0.2 nS *versus* 70 nS steady-state conductance).

Experiments at very low matrix protein concentrations under conditions of incomplete induction revealed that the smallest conductance that could be induced consisted of three unit steps

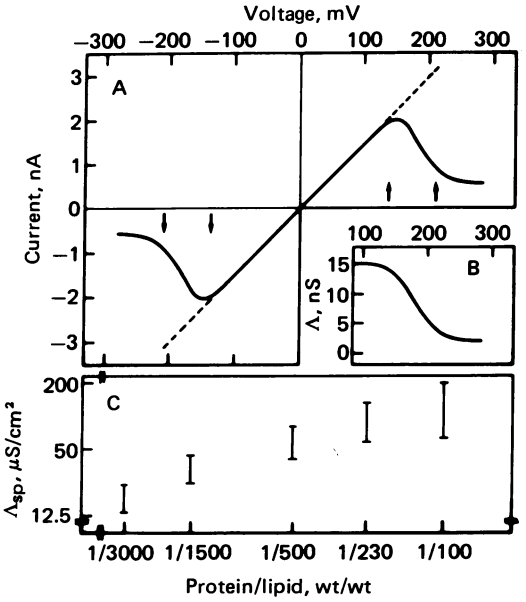

FIG. 2. (*A*) Current–voltage dependence. The solid line represents the steady-state current–voltage curve; the broken line is the instantaneous current–voltage dependence. The steady-state current–voltage curve was obtained between +280 mV and −280 mV by a continuous decrease of voltage (−20 mV/min). When the experiment was repeated in the opposite direction, no hysteresis was observed. The instantaneous current–voltage curve was recorded by voltage steps from 0 to final values between 5 and 300 mV (at intervals of 5 mV). Between measurements, 15 sec at 0 potential was allowed. The arrows at ±140 and ±210 mV indicate the positions of the potentials V_i and V_c at pH 7.4. V_i is defined as the potential generating an initial current response within an average of 10 min. Its value is pH-dependent (180 mV at pH 6 and 120 mV at pH 8). V_c is defined as the voltage above which higher potentials do not cause further initiation steps within 1 hr (values from 280 mV at pH 6 to 180 mV at pH 8). Partially induced membranes ($V_i < V_{applied} < V_c$) exhibited similar current–voltage curves at lower current values. (*B*) Conductance–voltage dependence, calculated from the steady-state current–voltage curve in A by using Ohm's law. (*C*) Dependence of specific conductance (Λ_{sp}) on protein-to-lipid ratios. Conductance values (Λ) were measured in fully induced membranes after reducing the voltage to 80 mV. The bars indicate the ranges of the observed values. The numbers of experiments (from left to right) were 3, 15, 17, 28, and 12.

(triplet), which appeared as a single increment during initiation, followed by a characteristic inactivation in three well-resolved decrements (Fig. 4). It should be noted also from this figure that, upon application of an extreme voltage increment (480 mV) to a single conductance unit, step heights occasionally change. Repeated applications of large increments to a single unit caused deviations that scattered around the unit step height with the same mean square deviation observed for entire populations of conductance units and without detectable discrete intermediate step heights. For instantaneous voltage increments not exceeding 300 mV or for continuous voltage application, the step heights of conductance remained unaffected.

Tracer flux across membranes

At pH values above 9.5, very high conductance levels arose spontaneously during membrane formation. Details of our observations under these conditions will be described elsewhere, but in the present context, this high conductance was exploited for quantitating the permeability properties of matrix protein containing membranes. Fig. 5 shows the increase in the glucose content of the recipient chamber of a membrane cell. After a

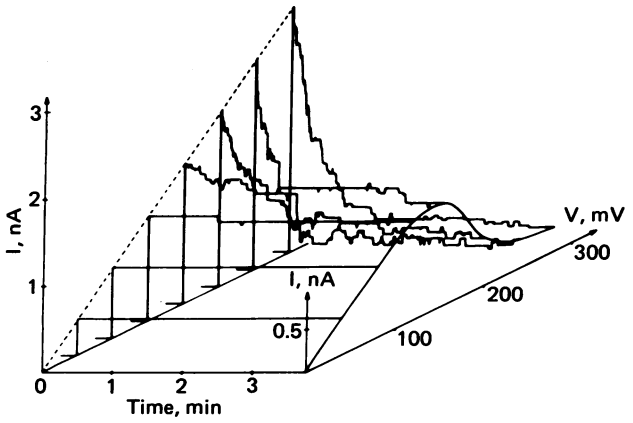

FIG. 3. Voltage dependence of current inactivation. The different traces were recorded with a fully induced membrane. After the voltage was set to zero, potentials of 40–280 mV were applied at intervals of 40 mV. The three-dimensional representation illustrates the ohmic relationship of the instantaneous current–voltage curve on the I and V axes on the left and the steady-state current–voltage curve after relaxation on the I and V axes on the right. Neither current decay nor fluctuations occur in the region below 80 mV, where instantaneous and steady-state currents coincide.

10-min delay, a linear increase with a slope of 0.42 fmol/min was observed. From Fick's law and the area of the entire bilayer, a permeability coefficient of 10^{-5} cm/s is obtained. Control experiments showed that glucose was not detected in the recipient chamber when induced membranes were used at pH 7.4. With membranes at pH 10 (conductance levels, 2–4 × 10^4 unit steps) and [^{3}H]inulin as the probe, no radioactivity was detected in the recipient chamber in three independent experiments of 60-min duration each.

DISCUSSION

The procedure used for the formation of matrix protein-containing planar lipid bilayers takes advantage of the efficient incorporation of protein into lipid vesicles (8). Conversion of vesicles into monolayers and the subsequent formation of membranes yield structures that, by all criteria applied, are bilayers. Their stability and, particularly, the high reproducibility of conductance measurements from sample to sample and from batch to batch are likely to be due to the reproducible composition of the monolayers, which do not contain residual

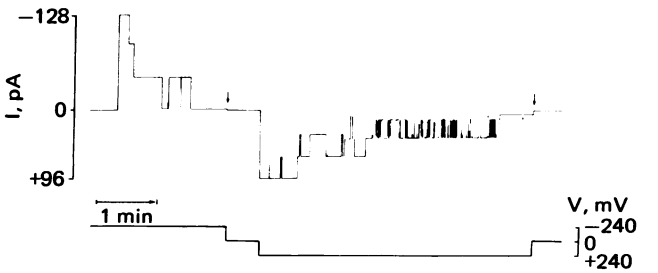

FIG. 4. Induction of conductance and inactivation at a very low protein-to-lipid ratio (1:3000, wt/wt) and incomplete initiation (240 mV at pH 6). The inactivation steps at −240 mV were 0.175 nS on average; after a single large voltage change to +240 mV, they were 0.12 nS. The step height change induced by the extreme voltage jump constitutes the largest we have observed. Also, note the residual currents after inactivation (arrows) and the rapid oscillation between two levels (amplitude, 0.1 nS). The latter suggests that, if unit step height is not reached, the current immediately returns to the level held previously (cf. also Fig. 1 *right*). Bandwidth, 100 Hz.

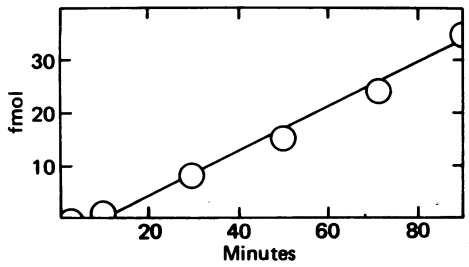

FIG. 5. Tracer flux. Bilayers (protein-to-lipid ratio, 1:3000, wt/wt) were generated in B buffer at pH 10. The conductance level (8×10^4 unit steps), monitored every 5 min at 20 mV, decreased 5% during the entire experiment. [^{3}H]Glucose (100 μCi), corresponding to 3 nmol, was applied to the donor chamber. Both chambers were stirred magnetically. At the times indicated, 200 μl (total chamber volume, 1 ml) was withdrawn and simultaneously replaced with buffer. Conversion of radioactivity to mole amounts took into account dilutions and quenching, but backdiffusion could be neglected. For the experiments with [^{3}H]inulin, its mass (M_r 5000) and monodispersity were confirmed by calibrated gel filtration.

detergents, hydrocarbon solvents, or membrane doping agents. Application of defined potentials to bilayers containing matrix protein results in membrane conductances that are caused by the presence of this protein. This conclusion is drawn from an approximately linear dependence of conductance levels on the protein concentration. All conductance changes observed occurred in well-resolved steps. Because analyses at both high and low conductance levels reveal that step heights are uniform in size and independent of voltage, we have operationally defined the smallest conductance increments observed as unit steps. From studies with ionophore antibiotics (24), it is well established that occurrence of discrete and uniform conductance changes is indicative of the opening and closing of ionic pathways, usually envisioned as single aqueous channels across the bilayer. This notion surely applied to matrix protein-containing membranes, because the current–voltage dependence of step heights is linear, the ion selectivity is poor, and small uncharged hydrophilic molecules can traverse the membrane across these channels.

Conductance steps may either reflect transitions between the open and closed states of individual channels or they may indicate discrete size variations of larger channels. The latter alternative has been demonstrated for alamethicin (22) and results in a hierarchy of step heights. If it were to apply to matrix protein channels, a range of step heights should also be observed, and inulin might pass through the larger channels. Because neither corollary is supported by our experimental data, we conclude that the conductance changes we observe are due to the opening and closing of channels of uniform size. The dependence of conductance on voltage can thus be attributed to the voltage-dependent transition of individual channels between two clearly distinct states. This is reflected macroscopically by the existence of two levels in the conductance–voltage relationship. At the high level, all channels would be open; they would be closed at low conductances (see below for a qualification of these statements). At intermediate levels, a voltage-dependent equilibrium exists between open and closed channels, because the conductances observed are independent of the pathway of approach. The effect of a potential corresponds to the closing of channels, a notion providing a microscopic interpretation of negative resistance and inactivation. Although apparently affording satisfactory explanations for the phenomena observed, it is likely that this two-state model represents a gross oversimplification. For instance, channels are probably inactive rather than closed prior to initiation, and residual conductances—e.g., the 2 nS at high potentials in membranes containing many channels (Fig. 2); persistence of residual conductance after inactivation of a channel triplet; cf. Fig. 4—imply a more complex picture.

An approximate diameter of matrix protein channels can be estimated from the unit step size of conductance, assuming that they are cylindrical in shape and filled with the aqueous solution present in the bulk phase. From the thickness of the matrix protein layer [4 nm; estimated from shadowed electron micrographs (6) and x-ray scattering data (unpublished data)] as the channel length, a diameter of about 1 nm is obtained. This value is in good agreement with an estimate derived from the results of our tracer flux studies. Because the permeability of uninduced membranes to glucose is negligible, we attribute the observed flux to open channels (about 50 molecules of glucose pass each channel per second). Their effective cross section for glucose diffusion can be calculated by using Fick's law. By assuming free diffusion of glucose in the channel, a value of 0.25 nm^2 is obtained which corresponds to an effective diameter of 0.55 nm. Because the total channel diameter is the sum of the effective diameter and the diameter of glucose (approximately 0.5 nm), this calculation yields a value of about 1 nm. The values obtained from ionic conductance and from glucose flux measurements thus are in reasonable agreement with each other and tally with the value derived from the exclusion size of oligosaccharides (1, 4). This consistency reinforces our conclusion that each unit step of conductance indeed corresponds to a single channel and demonstrates the validity of our assumption of essentially free diffusion of glucose across channels.

Our ultrastructural analyses (6) have shown a well-defined, rigid association of matrix protein subunits. The question therefore arises as to whether incorporation of this protein into lipid bilayers at concentrations far smaller than those occurring in the bacterial outer membrane* also leads to protein aggregates. This hypothesis is supported by the occurrence of delayed, large conductance increments during initiation, indicating the simultaneous activation of channel clusters rather than random activation of individual channels. More significantly, if channels open and close as independent units, the fluctuations at high conductance levels would yield standard deviations of an order of magnitude larger than the values observed. This result can be interpreted meaningfully only by postulating cooperativity among channels, which in turn implies protein–protein interactions. This leaves little doubt that the matrix protein assumes an aggregated state also in planar bilayers. The fact that neither loss nor gain of channels is observed over hours illustrates the conservation of these aggregates and their containment within lipid bilayer boundaries. This finding is matched by the insolubility of the matrix protein in aqueous solutions and the observation that it persists in highly aggregated form even if solvated in benzene or phenol (7). It will now be intriguing to ask whether the smallest conductance level observed reflects the arrangement of the matrix protein in the bacterial cell envelope: the former corresponds to three channels; the latter exhibits three-fold symmetry and shows, as one of the most prominent features, triplet indentations (6).

* At protein-to-lipid ratios of 1:500 (wt/wt), the protein content is 1000-fold lower in the area of the bilayer (0.02 mm^2) than in the bacterial envelope (6). From the permeability coefficient (10^{-5} cm/sec; cf. *Results*), one, therefore, would expect a value of 10^{-2} cm/sec for bacterial cells. This is close to that (1.4×10^{-2} cm/s) observed in whole *E. coli* cells (25). Thus, the ratio of open to closed channels (1:20) in the artificial bilayer is similar to that in bacterial cells. At pH 6–8, the fraction of open channels is about 1% of the above value.

Of course, many questions remain unresolved. Why are matrix protein channels voltage-controlled, and what is the mechanism of this process? Why is the fraction of active, open channels in the bacterial cell similar* to that in bilayers at pH 10, whereas it is substantially smaller in planar bilayers at physiological pH? Channel induction is voltage-dependent between pH 6 and 8 but is spontaneous at pH 10. Could the high pH reduce an energy barrier that may prevail in the lipid bilayer at the lower pH? Many components of the bacterial envelope are absent in artificial membranes. What is the role of other proteins, of the peptidoglycan, and of the highly charged lipopolysaccharides that exist in outer membranes in much larger amounts than found tightly associated with the matrix protein? Furthermore, the conclusion that the matrix protein forms arrays of interacting channels, whose two-state distribution is dependent on voltage, also raises new questions. Perhaps the most intriguing one is whether the closing of channels by high potentials could have evolved as a mechanism to allow the regulation of outer membrane permeability. If this hypothesis were correct, the large fraction of closed channels would be the result of a potential across the outer membrane that locally may be above the measured average value (26), possibly due to the asymmetrical charge distribution at the outer membrane (27). Of course, there may be other and perhaps more trivial reasons that could entail a voltage dependence merely as a by-product. Yet, these questions have correlates in other proteins, such as the excitability-inducing material (28) and in those proteins involved in gating processes in general (29). We therefore believe that the matrix protein merits further study. It will also be interesting to determine whether the method used to incorporate it into planar bilayers will be applicable to other proteins.

Note Added in Proof. Benz *et al.* (30) have incorporated matrix protein into preformed planar membranes in the presence of docecyl sulfate or cholate. Despite the differences in methods and membrane composition, they obtained results that are consistent with the formation of aqueous channels with a diameter of 0.9 nm.

We thank Drs. G. Schwarz and M. Zulauf for stimulating discussions and Drs. T. Bickle, G. Schatz, J. Seelig, and A. Steven for critical reading of the manuscript. Dr. M. Zulauf kindly performed the coherent light scattering experiment and J. Bietenhader and M. Regenass provided expert technical assistance. This investigation was supported by Grants 3.152-0.77 and 3.059-0.76 from the Swiss National Science Foundation.

1. Nakae, T. (1976) *Biochem. Biophys. Res. Commun.* **71,** 877–884.
2. Henning, U., Lugtenberg, E. J. J., Mizushima, S., Rosenbusch, J. P. & Schnaitman, C. A. (1978) *J. Bacteriol.*, in press.
3. Di Rienzo, J. M., Nakamura, K. & Inouye, M. (1978) *Annu. Rev. Biochem.* **47,** in press.
4. Nikaido, H. (1976) *Biochim. Biophys. Acta* **433,** 118–132.
5. Rosenbusch, J. P. (1974) *J. Biol. Chem.* **249,** 8019–8029.
6. Steven, A. C., ten Heggeler, B., Mueller, R., Kistler, J. & Rosenbusch, J. P. (1977) *J. Cell Biol.* **72,** 292–301.
7. Rosenbusch, J. P. & Mueller, R. (1977) in *Solubilization of Lipo-Protein Complexes,* eds. Peeters, H. & Massue, J. P. (European Press, Ghent, Belgium), pp. 59–68.
8. Racker, E., Knowles, A. F. & Eytan, E. (1975) *Ann. N. Y. Acad. Sci.* **264,** 17–33.
9. Montal, M. (1976) *Annu. Rev. Biophys. Bioeng.* **5,** 119–135.
10. Takacs, B. J. & Rosenbusch, J. P. (1975) *J. Biol. Chem.* **250,** 2339–2350.
11. Cubero Robles, E. & Van Den Berg, D. (1969) *Biochim. Biophys. Acta* **187,** 520–526.
12. Arvidson, G. A. E. (1965) *J. Lipid Res.* **6,** 574–577.
13. Kuksis, A. (1967) in *Lipid Chromatographic Analysis,* ed. Marinetti, B. V. (Dekker, New York), p. 279.
14. Ames, B. N. & Dubin, D. T. (1960) *J. Biol. Chem.* **235,** 769–775.
15. Huang, C. (1969) *Biochemistry* **4,** 344–352.
16. Zulauf, M. (1977) *J. Mol. Biol.* **114,** 259–266.
17. Verger, R. & Pattus, F. (1976) *Chem. Phys. Lipids* **16,** 285–291.
18. Phillips, M. C., Hauser, H. C. & Paltauf, F. (1972) *Chem. Phys. Lipids* **8,** 127–133.
19. Schindler, H. & Feher, G. (1976) *Biophys. J.* **16,** 1109–1113.
20. Montal, M. & Mueller, P. (1972) *Proc. Natl. Acad. Sci. USA,* **69,** 3561–3566.
21. Benz, R., Fröhlich, O., Läuger, P. & Montal, M. (1975) *Biochim. Biophys. Acta* **394,** 323–334.
22. Boheim, G. & Kolb, H. A. (1978) *J. Membr. Biol.* **38,** 99–150.
23. Prehm, P., Stirm, S., Jann, B. & Jann, K. (1975) *Eur. J. Biochem.* **56,** 41–55.
24. McLaughlin, S. & Eisenberg, M. (1975) *Annu. Rev. Biophys. Bioeng.* **4,** 335–366.
25. Bavoil, P., Nikaido, H. & Meyenburg, K. (1977) *Mol. Gen. Genet.* **158,** 23–33.
26. Stock, J. B., Rauch, B. & Roseman, S. (1977) *J. Biol. Chem.* **252,** 7850–7861.
27. Mühlradt, P. F. (1976) *J. Supramol. Struct.* **5,** 103–108.
28. Mueller, P. & Rudin, D. O. (1963) *J. Theor. Biol.* **4,** 268–280.
29. Stevens, C. F. (1977) *Nature* **270,** 391–396.
30. Benz, R., Janko, K., Boos, W. & Läuger, P. (1978) *Biochim. Biophys. Acta,* in press.